AIP | Applied Physics Letters

Lasing in a metal-clad microring resonator

Min W. Kim and P.-C. Ku

Citation: Appl. Phys. Lett. **98**, 131107 (2011); doi: 10.1063/1.3573818
View online: http://dx.doi.org/10.1063/1.3573818
View Table of Contents: http://apl.aip.org/resource/1/APPLAB/v98/i13
Published by the AIP Publishing LLC.

Lasing in a metal-clad microring resonator

Min W. Kim[a] and P.-C. Ku[b]
Department of Electrical Engineering and Computer Science, University of Michigan, 1301 Beal Ave., Ann Arbor, Michigan 48109, USA

(Received 7 December 2010; accepted 14 March 2011; published online 29 March 2011)

Metal cladding was experimentally demonstrated to be a feasible method to further scale down the size of a microring laser. Shrinking the physical dimensions of semiconductor microring resonators has been difficult due to a large waveguide bending loss. We experimentally show that light can be better confined into a much tighter space by using the plasmonic metal structure, thereby enabling miniaturization of a microring laser. © *2011 American Institute of Physics*. [doi:10.1063/1.3573818]

Semiconductor microring resonators have been widely used as a fundamental building block for photonic integrated circuits.[1–3] Semiconductor lasers employing microring cavities exhibit unique advantages that include traveling-waves which require no need for additional feedback structures such as mirrors, convenient out-coupling to in-plane waveguides, and independent control of the emission wavelength from the device size. Furthermore, nanoscale ring laser devices can enable a single longitudinal mode operation and tighter integration between electronic and photonic components. To date, however, physical dimensions of state-of-the-art microring lasers remain at diameters greater than 7.5 μm (Ref. 4) due to large waveguide bending loss in a small ring resonator.[5] Recently, use of plasmonic structures in photonic components has led to nanoscale waveguides,[6] photodetectors,[7] and lasers.[8–15] In these devices, light penetrates little into the metal layer and can, therefore, be confined in a much tighter space. State-of-the-art subwavelength lasers that employ metal structures include bowtie cavity lasers,[8,9] metal-clad nanopillar and Fabry–Perot lasers,[10,11] plasmonic nanowire lasers,[12] spacer-based nanolasers,[13] and metal-optic nanopatch laser.[15] In this letter, we report an experimental demonstration using a 4 μm diameter ring resonator confirming the integration of metal and ring resonators can lead to coherent oscillation that was otherwise difficult to attain.

A metal-clad semiconductor microring resonator is a semiconductor microring resonator conformally clad with plasmonic metal. The semiconductor part of the metal-clad resonator is illustrated in Fig. 1(a) with a cross-sectional view shown in Fig. 1(b). Metal surrounding the semiconductor enhances the optical confinement since the electric field rapidly goes to zero inside the metal. The lateral and transverse optical modes are purely dielectric and hybrid dielectric-plasmonic in nature, respectively. The hybrid nature of the transverse optical mode, as shown in Fig. 1(b), provides an enhanced optical confinement, although at the loss of increased metal dissipation. A detailed analysis is required to optimize the trade-off between the added optical confinement and the metal loss and will be presented elsewhere. This letter will focus on the experimental demonstration that showed an increased cavity quality (Q) factor as a result of enhanced optical confinement due to the metal cladding, which outweighed added metal loss. Therefore, the metal cavity can provide a feasible pathway for continued scaling of a microring laser.

A metal-clad microring laser structure, as shown in Fig. 2(a), consisting of a bulk InGaAsP active region that is lattice-matched to InP, was epitaxially grown by metal-organic chemical vapor deposition. The two InP layers serve as waveguide cladding layers for transverse optical confinement. The top n^+-InGaAs and bottom p^+-InGaAsP were also included for future electrical injection. The device was patterned by e-beam lithography and reactive ion etching. Raith 150 electron-beam lithography system was used to define the rings using a bilayer polymethyl methacrylate (PMMA) structure to enhance the subsequent lift-off process. MicroChem 495K A6 PMMA develops away faster than MicroChem 950K A2 PMMA, thereby providing a negative angle for lift-off. 50 nm of titanium (Ti) was deposited using electron beam evaporation and lifted off in acetone. Using Ti as the mask, the InGaAsP/InP epiwafer was dry etched in a $CH_4/H_2/Ar$ [4 SCCM (SCCM denotes cubic centimeter per minute at STP)/28 SCCM/14 SCCM] environment, in PlasmaTherm 790. The pressure and power were maintained at 30 mTorr and 200 W, respectively. During the InP etching, polymer was deposited as a by-product and was removed using an O_2 ashing cycle (70 SCCM, 200 mTorr, 100 W, 3 min). A scanning electron micrograph showing the device after the aforementioned etching steps is in Fig. 2(b). The total height of the microring resonator was 1100 nm and the sidewall angle was 84.5°. Afterward, a thin (20 nm) layer of gold (Au) was deposited using electron beam evaporation as a seed layer for the subsequent electrodeposition step. In total, 320 nm of Au was deposited. It has been discovered

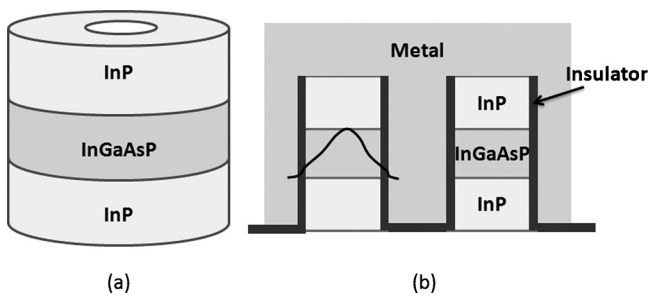

FIG. 1. (a) 3D schematic of a semiconductor microring resonator (without metal cladding). (b) Cross-sectional view of the metal-clad semiconductor microring resonator.

[a]Author to whom correspondence should be addressed. Electronic mail: minwkim@umich.edu. FAX: 1-734-764-7134.
[b]Electronic mail: peicheng@umich.edu.

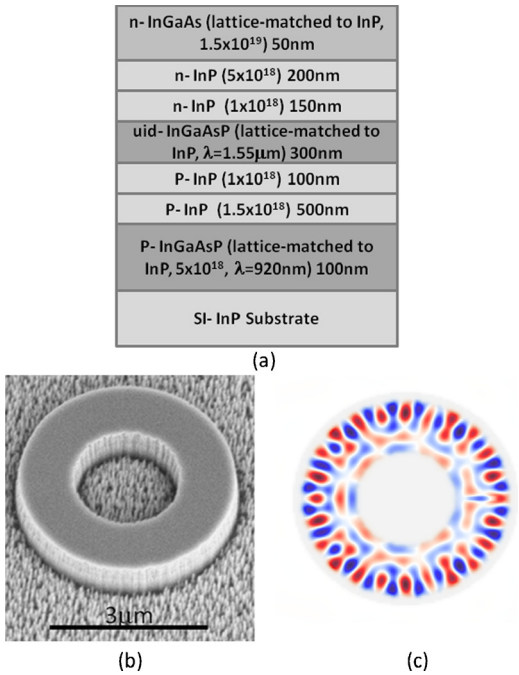

FIG. 2. (Color online) (a) The epitaxial structure of the metal-clad microring resonator. (b) Scanning electron micrograph showing a 4 μm diameter ring laser after etching, before metal coverage. (c) 3D FDTD simulation of the laser device shown in (b) at resonance. The whispering gallery mode is clearly shown.

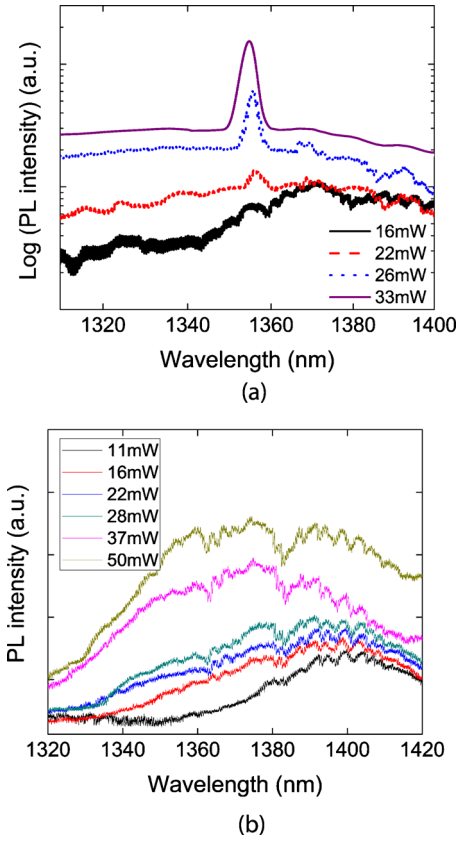

FIG. 3. (Color online) Intensity-dependent μ-PL of a 4 μm microring resonator, (a) covered with Au and (b) not covered with Au, that was measured at T=77 K. The power shown in the legend is the output power from the pump laser. Only a small fraction (<1%) of the power indicated in the legend is absorbed by the device.

that the lack of an insulator layer between the semiconductor and gold does not prevent the resonator from lasing for a microring resonator with dimensions much larger than a wavelength. However, as the device dimensions become closer to subwavelength, such an insulator layer plays a greater role in separating electric field from the metal such that photoluminescence quenching does not occur. A three-dimensional (3D) finite-difference-time-domain (FDTD) simulation predicts the electric field shown in Fig. 2(c) for a metal-clad ring laser whose dimensions match the one shown in Fig. 2(b). This clearly shows that the device operates in the whispering gallery mode. The mode volume of the device was calculated to be 0.7 μm^3, which corresponds to $0.32\lambda^3$, where λ is the lasing wavelength in free-space.

Intensity-dependent microphotoluminescence (μ-PL) was measured at 77 K for both metal-covered and pure dielectric ring resonator cavities of the same diameter (4 μm) and ring width (1 μm). They were optically pumped through the InP substrate using a 1064 nm wavelength continuous-wave pump laser. In order to align the pump laser with the devices, the gold outside of the device region was etched away using optical lithography for the metal-covered ring resonators. In addition, to facilitate pumping through the substrate, the InP substrate was polished. A 20× long-working-distance objective lens was used to focus the pump laser onto the laser devices. Figure 3(a) shows the intensity-dependent μ-PL of the metal-clad microring resonator. The transition from a spontaneous emission to a single-peak stimulated emission can be clearly seen at 21.5 mW pump power which corresponds to 1.2 mW of power absorbed by the active region assuming a 6 μm diameter of laser focusing spot. The actual absorption should be even lower due to substrate roughness and reflection from cryostat window. On the other hand, Fig. 3(b) shows the intensity-dependent μ-PL of the 4 μm diameter pure dielectric ring resonator. Although there was a shoulder developing near the region in which there was a single lasing peak for the device with Au coverage, it never fully developed into a stimulated emission peak. We attribute this difference to the fact that higher confinement factor for the device with Au coverage decreases the leakage of field as it travels around the ring, which increases both the cavity-Q factor and modal gain.

Figure 4(a) shows the L-L curve of the peak μ-PL intensity. The ring resonator that is covered with Au (in black) shows the transition from a spontaneous emission to a stimulated emission at the threshold. On the other hand, the device that is not covered with Au (in red) shows no such transition. Figure 4(b) shows the full-width half-maximum (FWHM) linewidth and the peak wavelength of the stimulated emission for the metal-clad microring laser. The linewidth collapses at the laser threshold from 8 nm down to 1.77 nm. Additionally, the emission peak wavelength, at first, increases due to sample heating as the pump intensity becomes larger. However, when it reaches lasing, the peak starts to blueshift, possibly due to frequency pulling.[14]

We also fitted the spontaneous emission factor β of the metal-clad microring laser using the following rate equations:[15]

$$\frac{dN}{dt} = P - gS - \frac{1-\beta}{\tau_{sp}}N - \frac{F\beta}{\tau_{sp}} - \frac{v_s S_a}{V_a}N,$$

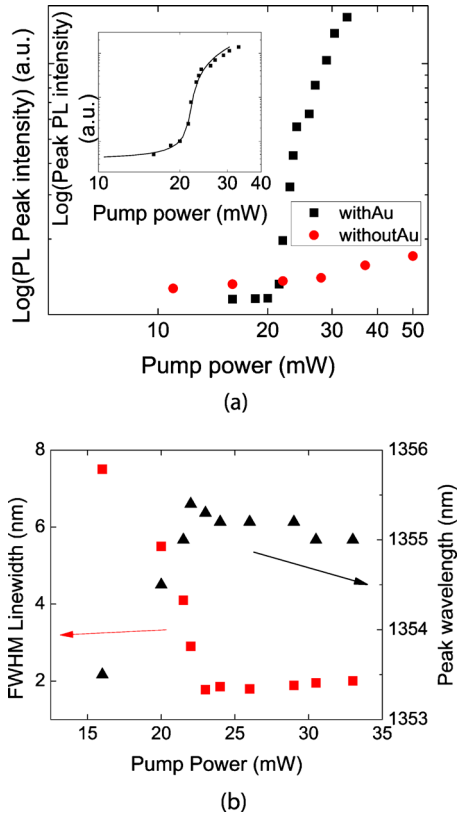

FIG. 4. (Color online) (a) Comparison of peak intensity vs pump power for 4 μm ring laser devices covered with Au and not covered with Au. Inset: peak PL intensity vs pump power for metal-clad microring laser. The line was fitted using the laser rate equations with the Purcell factor taken into account. (b) FWHM and peak wavelength of the lasing peak of a 4 μm microring laser device covered with Au at various pump powers. Lines are for visual guidance only.

$$\frac{dS}{dt} = \Gamma g S - \frac{S}{\tau_{ph}} + \frac{\Gamma F \beta}{\tau_{sp}} N,$$

where N and S are carrier and photon densities, P is the pumping rate, g is the optical gain, τ_{sp} is the spontaneous emission lifetime ($\tau_{sp}=1.5$ ns), F is the Purcell factor, S_a and V_a are exposed surface area and volume of gain region ($S_a=2\pi r_{out}h+2\pi r_{in}h$, $V_a=\pi r_{out}^2 h-\pi r_{in}^2 h$), respectively, v_s is surface recombination velocity ($v_s=2\times10^4$ cm/s), Γ is confinement factor ($\Gamma=0.65$), and τ_{ph} is the photon lifetime ($\tau_{ph}=Q/2\pi f$, where f is the resonant frequency). g was assumed to follow a linear model with $g=cG(N-N_o)/n_g = 1.09\times10^{-5}(N-4\times10^{17})$ s^{-1}, where N_o, c, n_g, and G are the transparent carrier density, light velocity in vacuum, the group refractive index of the cavity, and the linear differential gain coefficient, respectively. The Purcell factor was calculated to be 1.32 with a Q factor of 160, determined experimentally from far below the lasing threshold, and the calculated mode volume. The theoretical Q factor value from a 3D FDTD simulation yielded 331. Although it is expected that Q factor should be even higher at lower temperatures due to decreased phonon scattering, the actual lower Q factor could be attributed to rough and angled sidewalls. For simulation purposes, n and k values of Au from Ref. 16 were used. The β factor was found to be 5×10^{-4}.

In summary, we have demonstrated lasing in a metal-clad semiconductor microring resonator. The metal cladding allowed one to achieve coherent emission from a small microring resonator that was otherwise difficult to attain. A similar ring resonator without metal cladding did not transition from spontaneous to stimulated emission. This result demonstrated a strategy to continue the scaling of a microring laser.

This work was supported by the DARPA/MTO NACHOS program (Grant No. W911NF-07-1-0313) and was partially performed in the Lurie Nanofabrication Facility, which is part of the NSF NNIN network.

[1] A. S.-H. Liao and S. Wang, Appl. Phys. Lett. **36**, 801 (1980).
[2] A. W. Poon, X. S. Luo, F. Xu, and H. Chen, Proc. IEEE **97**, 1216 (2009).
[3] F. Xia, L. Sekaric, and Y. Vlasov, Nat. Photonics **1**, 65 (2007).
[4] J. Van Campenhout, P. Rojo-Romeo, P. Regreny, C. Seassal, D. Van Thourhout, S. Verstuyft, L. Di Cioccio, J.-M. Fedeli, C. Lagahe, and R. Baets, Opt. Express **15**, 6744 (2007).
[5] D. Marcuse, *Theory of Dielectric Optical Waveguides*, 2nd ed. (Academic, San Diego, CA, 1991).
[6] M. I. Stockman, Phys. Rev. Lett. **93**, 137404 (2004).
[7] E. Laux, C. Genet, T. Skauli, and T. W. Ebbesen, Nat. Photonics **2**, 161 (2008).
[8] N. Yu, E. Cubukcu, L. Diehl, D. Bour, S. Corzine, J. Zhu, G. Hofler, K. Crozier, and F. Capasso, Opt. Express **15**, 13272 (2007).
[9] S. W. Chang, C. Y. Ni, and S. L. Chuang, Opt. Express **16**, 10580 (2008).
[10] M. T. Hill, Y.-S. Oei, B. Smalbrugge, Y. Zhu, T. De Vries, P. J. Van Veldhoven, F. W. M. Van Otten, T. J. Eijkemans, J. P. Turkiewicz, H. De Waardt, E. Jan Geluk, S.-H. Kwon, Y.-H. Lee, R. Notzel, and M. K. Smit, Nat. Photonics **1**, 589 (2007).
[11] M. T. Hill, M. Marell, E. S. P. Leong, B. Smalbrugge, Y. Zhu, M. Sun, P. J. Van Veldhoven, E. Jan Geluk, F. Karouta, Y.-S. Oei, R. Notzel, C.-Z. Ning, and M. K. Smit, Opt. Express **17**, 11107 (2009).
[12] R. F. Oulton, V. J. Sorger, T. Zentgraf, R.-M. Ma, C. Gladden, L. Dai, G. Bartal, and X. Zhang, Nature (London) **461**, 629 (2009).
[13] M. A. Noginov, G. Zhu, A. M. Belgrave, R. Bakker, V. M. Shalaev, E. E. Narimanov, S. Stout, E. Herz, T. Suteewong, and U. Wiesner, Nature (London) **460**, 1110 (2009).
[14] A. Yariv, *Optical Electronics* (Saunders College, Philadelphia, 1991), p. 180.
[15] K. Yu, A. Lakhani, and M. C. Wu, Opt. Express **18**, 8790 (2010).
[16] P. B. Johnson and R. W. Christy, Phys. Rev. B **6**, 4370 (1972).